Development of Continuous Flow Analysis System Based on Amperometric Biosensors

***Abstract*—Although the basic theory for electrochemical measurement is well known, there is still much to be developed in specific instrumental systems for biosensors, especially to achieve fast response times, usefulness, and low-cost equipment. In this regard, continuous flow analysis (CFA) systems with an integrated biosensor are valuable tools for bioanalysis monitoring. These systems are suitable for automation and monitoring in real time with a short response time. Among biosensors, amperometric ones are the most used due to their high selectivity and wide linear range. In this work, we design and develop all parts of an automated CFA system for bioanalysis based on amperometric biosensors. It consists of several inlets for the samples, standards, and carrier solution; a fluidic subsystem; an electronic subsystem in which output voltage will be directly correlated to the analyte concentration in the solution; and a software application to configure and control all the features of the system. The prototype was successfully validated using an amperometric biosensor to analyze the ethanol content of low-alcohol beers.**

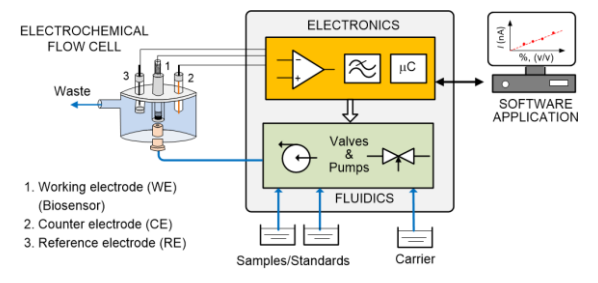

I. Introduction

In recent years, researchers have made great efforts in employing biosensors to develop automated systems for continuous bioanalysis. The integration of biosensors in these kinds of systems requires reliable biosensors with the necessary specificity and sensitivity and developing robust and accurate instrumental systems.

A biosensor is defined [1,2] as a compact analysis device that includes a biological recognition element (nucleic acid, enzyme, antibody, tissue, cell, etc.) associated with a transduction system that allows the processing of the signal produced by the interaction between the recognition element and the analyte. This signal is later amplified and processed to extract the analyte concentration. Fig. 1 shows a typical biosensor setup. Some of the most used biological recognition elements (receptors) are enzymes that exhibit a very high catalytic activity and have a high selectivity. The typical transducers in the development of biosensors are undoubtedly electrochemical. This is due to the advantages they bring, including the ability to measure small volumes, the signal generated being electrical, the detection limits being suitable for the detection of many analytes, and the instrumentation being simple and inexpensive. The most promising electrochemical sensors are amperometric biosensors [3], which measure the currents resulting from the oxidation or reduction reactions between the biological element and an electrode. In these kinds of biosensors, the quantity of the analyte present in the sample is generally linear to the electrical current generated by the electrochemical reaction. This behavior requires a constant differential voltage between electrodes. This voltage is typical between –0.6 and +0.9 V, depending on the specific biosensor.

Over the years, various approaches have been made in bioanalysis monitoring, such as flow injection analysis [4–8], continuous flow analysis (CFA) [9,10], sequential injection [11,12], and multi-commutation flow [13,14]. These techniques have been implemented using distinct methods, including spectrometric [15], optical [16], and electrochemical measurements [17]. Most of these methods can monitor the concentration of analytes in real time [18]. However, the application of these systems to food and drink industrial production is still a challenge because they need to be used for continuous monitoring and quick response times.

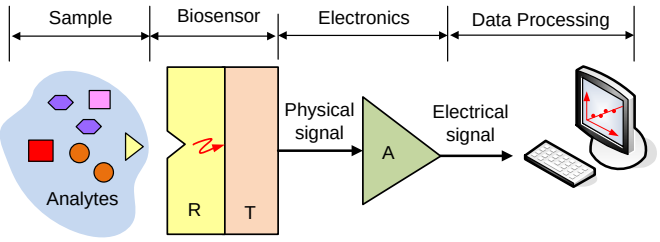

Fig 1. Biosensor setup: R=Receptor; T=Transducer; A=Amplifier.

This work was supported in part by Spanish Government (Inter-Ministerial Commission of Science and Technology) under the Grant CC-04-PTR1995-0783-0P.

A. López, F.J. Ferrero, M. Valledor, and J.C. Campo are with the University of Oviedo, 33204, Spain (e-mail: ferrero@uniovi.es).

J. Reviejo and J.M. Pingarrón are with the Complutense University of Madrid, 28040, Madrid, Spain (reviejo@quim.ucm.es).

CFA is a powerful tool to take advantage of the continuous monitoring of samples, possible automation, fast response times, and the specificity of amperometric biosensors. It consists of transporting a controlled number of samples to the biosensor. When the sample reaches the amperometric biosensor, an electrical current is generated that is proportional to the analyte concentration in the sample. To control the flow of samples, standards, and the carrier through the system, several actuators (valves and micro pumps) were used, which will be activated according to a time diagram defined by the user.

The main contribution of this work is the design and development from the basis of all key components of an automated CFA system. It can be used in drink (beers and wines) industries to determine the content of a specific target analyte.

The structure of the paper is organized as follows. In Sec. II, we describe the materials and methods used. Sec. III is devoted to the experimental results, including several mechanical issues. Finally, Sec. IV provides the conclusion.

II. Materials and Methods

The developed CFA system can be considered divided into four functional blocks: fluidic subsystem, electronic subsystem, electrochemical flow cell, and software application, which are depicted in Fig. 2.

A. Fluidic Subsystem

The fluidic subsystem consists of seven inlets for the samples and standards, one input for the carrier solution, and one outlet for waste. To control the flow of samples, standards, and the carrier, ten solenoid valves and two peristaltic micro pumps were used, as shown in Fig. 3. Valves 1–7 are used to transport the samples and the standards to the fluidic circuit. Valves 8–10 are used to transport the carrier solution to the pumps. The peristaltic tubing pumps were selected to operate with a flow rate of less than 2 ml/min. One pump fills the loop with the standard solution, and the other transports the carrier solution, or the volume contained in the loop, to the flow cell. The loop is employed to make sure the fluidic circuit is never empty. The waste outlet is used to eliminate the excess sample in the filling loop, for cleaning the circuit, or for changing the inlet.

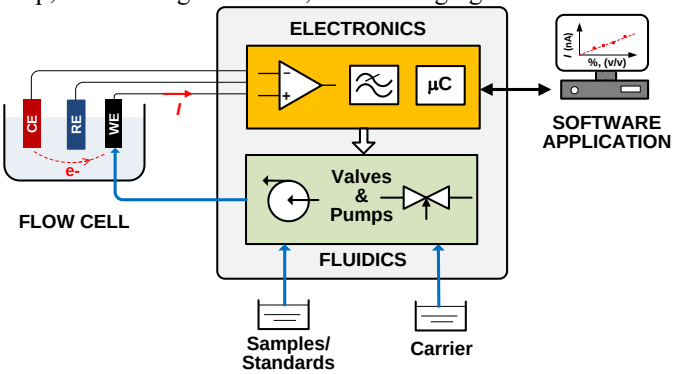

Fig 2. General view of the proposed CFA system based on amperometric biosensors. RE=Reference electrode; WE=Working electrode; CE=Counter electrode; µC=microcontroller.

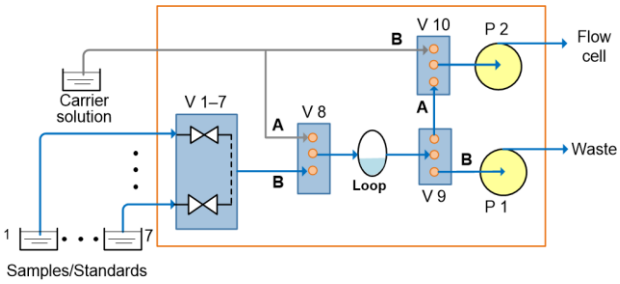

Fig 3. Fluidic subsystem. Electrovalves 1–7 are 1-way model WTA-2-8MFF from Takasago Electric Company. Electrovalves 8–10 are 2-way model WTB-3R-N3F1 from the Takasago Electric Company. Peristatic pumps are provided by the Welco Company, model WPM1-S2AB-RP.

The timing diagram of the fluidic subsystem consists of three phases: stabilizing, filling, and emptying. These phases are established by the user in the software application.

The stabilizing happens only when the instrument is connected. During this phase, a carrier is introduced into the electrochemical flow cell for cleaning the rest of the previously analyzed substance. During the filling phase, valves 8, 9, and 10 are open at inlet B, and at the same time, pumps 1 and 2 are functioning. Pump 1 carries the excess fluid to the waste outlet, and pump 2 carries the fluid to the electrochemical cell. The loop takes 50 seconds to fill, and the rest of the time, it is used to inject buffer solution into the flow cell. During the emptying phase, valves 8, 9, and 10 are open at inlet A. During this stage, only pump 2 is working. The carrier pushes the sample or standard from the loop to the electrochemical cell for 10 seconds. The rest of the time, a buffer solution is being injected into the cell to remove the concentration of the substance that is being analyzed.

Fig. 4 depicts some details of the fluidic circuit. Fig. 4 (a) shows the loop made using a 1.5 mm tube. During the operation, bubbles can reach the biosensor, which can be seen in Fig. 4 (b). This issue, caused by a poor union in the pipes, can produce measurement errors. To solve this problem, a thin copper wire is wound around the pipes to prevent air from entering the fluidic circuit, Fig. 4 (c).

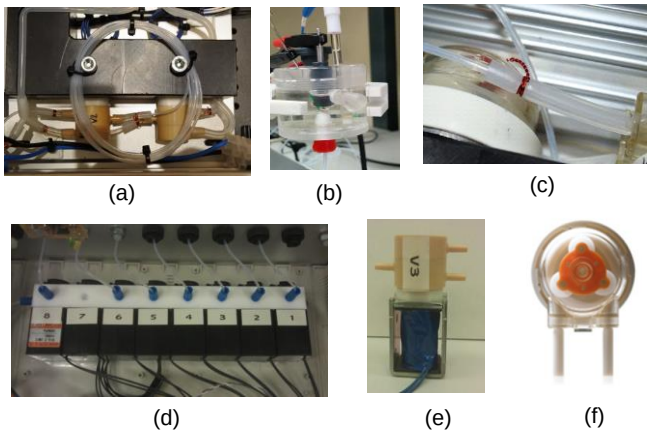

Fig 4. Details of the fluidic circuit: (a) Loop; (b) Electrochemical flow cell showing a bubble near the biosensor; it has a cylindrical shape and was made of methacrylate, with a capacity of 40 ml; (c) Wire of copper around the pipes; (d) Ensemble of 1-way solenoid valves; (e) 2-way solenoid valve; (f) Peristaltic tubing pump.

B. Electrochemical Flow Cell and Electrodes

The electrochemical flow cell contains three electrodes: the working electrode (WE), the reference electrode (RE), and the counter electrode (CE). The WE is the biosensor itself, where the electrochemical reaction is produced. The research group from the Complutense University of Madrid has developed enzymatic biosensors mainly for alcohol, glucose, fructose, cholesterol, and L-lactate [19–21]. We employed a composite graphite-Teflon ethanol biosensor developed previously in our research group [19]. This biosensor can be easily reused by polishing its surface [22]. The RE was a BAS Ag/AgCl/KCl model MF-2052, and the CE was a platinum wire. Fig. 5 (a) is a real picture of the biosensor, and Fig. 5 (b) shows the electrode reactions of the ethanol determination. Alcohol oxidase oxidizes ethanol to acetaldehyde using oxygen (O_2) as the electron acceptor, producing hydrogen peroxide (H_2O_2) as a by-product. Subsequently, HRP enzyme reduces H_2O_2 to H_2O, using ferrocene as an electron donor and producing ferrocenium. The measured cathodic current corresponded to the electrochemical reduction of generated ferrocenium and is proportional to the ethanol concentration.

For amperometric biosensors, the area of the working electrode and the scanning rate will affect the measurement results. The smaller the contact surface between donor and acceptor solutions, the lower the amount of ethanol that reached the detector. In this work, a contact surface diameter of 10 mm and one PTFE membrane of 0.45 µm pore diameter were chosen because they provided an adequate sensitivity for the analysis of beers with an ethanol concentration below 1.0% (v/v). By contrast, the scanning rate, defined as the frequency at which the complete measurement of a sample is carried out, depends on the suitable operation of the biosensor and the analysis method and settings established from the system configuration. In this work, the ethanol concentration is monitored every second in time intervals of 1 h, this being a programmable parameter.

To design the amperometric detector, must be considered a model of the electrochemical. Fig. 5 (c) shows the model of the cell used in this work [23]. It includes a solution resistance (R_1), a double layer capacitor (C_2), and a charge transfer or polarization resistance (R_2).

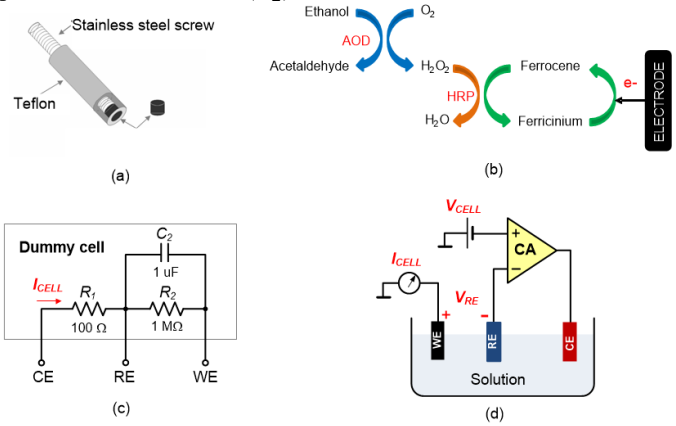

Fig 5. (a) Graphite-/Teflon-/AOD-/HRP-/ferrocene composite electrodes to alcohols; (b) Electrode reactions involved in the ethanol biosensor; (c) A simple equivalent circuit of an electrochemical cell; (d) Principle of a controllable electrochemical cell.

The transfer function of this circuit can be obtained from (1) to (6):

$$Z_T = \frac{sC_2R_1R_2 + R_2}{1 + sR_2C_2} \quad (1)$$

$$I_{CELL} = \frac{V_{CE}(s) - V_{WE}(s)}{Z_T} \quad (2)$$

$$V_{CE}(s) - V_{RE}(s) = I_{CELL}R_1 \quad (3)$$

$$V_{RE}(s) = G_1(s)V_{CE}(s) + G_2(s)V_{WE}(s) \quad (4)$$

$$G_1(s) = \frac{R_1}{sC_2R_1R_2 + R_1 + R_2} \quad (5)$$

$$G_2(s) = \frac{R_1(sC_2R_2 + 1)}{sC_2R_1R_2 + R_1 + R_2} \quad (6)$$

where $G_1(s)$ and $G_2(s)$ represent the influence of the CE and WE on the RE. Because we want to control the RE, $G_2(s)$ can be interpreted as interference.

Fig. 5 (d) shows the principle of a controllable electrochemical cell [24,25]. The control amplifier (CA) compares the potential difference between WE and RE with the desired cell voltage, V_{CELL}. The CA provides adequate current to maintain a constant voltage between WE and RE. Unfortunately, a real circuit requires additional elements, which will be introduced in the next subsection.

C. Electronic Subsystem

The electronic subsystem has been divided into two printed circuits boards (PCBs): (1) an amperometric detector to measure the electrical current generated in the flow cell and to control the electrochemical cell and (2) a circuit to drive the actuators of the fluidic circuit.

1) Amperometric Detector: The amperometric detector can be developed using different approaches. In [26], the authors provide an excellent review about electronics for amperometric biosensors. [27,28] are low-cost systems for portable electrochemical detection. [29] is a telemetry system for amperometric biosensors. [30] presented is a single-ended potentiostat topology for amperometric chemical sensors, and [31] is a fully differential potentiostat. In [32], the authors report a single chip potentiostat based on a programable system. Finally, [33] presents an innovative device for IoT biosensors.

In this work, we propose a versatile amperometric detector that can easily be adapted to different kinds of amperometric biosensors. Fig. 6 is a simplified block diagram of the amperometric detector. It consists of three functional parts: the current measurement circuit, the voltage measurement circuit, and the control amplifier, which will be described below.

The cell current, I_{CELL}, is measured by a typical current-to-voltage converter (I/V converter), with different resistors in the feedback loop for changing the current scale from nA to µA. To phase compensation and filter out high noise, a small capacitor in parallel with each resistor is needed. A shift voltage V_{BIAS} is added at the non-inverting input of the operational amplifier OA2 for measuring negative currents from the biosensor. The current measurement circuit must measure low current levels. Therefore, the criteria were to choose an operational amplifier (Op) with very low input bias and high input impedance. These

parameters should be very large to minimize any current losses through this stage.

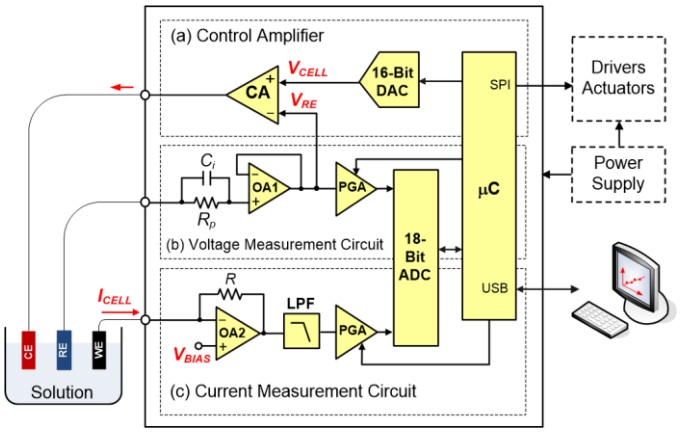

Fig 6. Block diagram of the amperometric detector: µC=PIC18F4550; OA1=OPA140; OA2=OPA4364; ADC=MCP3422; DAC=DAC8751.

After the I/V converter, there is a low-pass antialiasing filter, a programmable gain amplifier (PGA), and an 18-bit ADC. The microcontroller (µC) selected the gain of the PGA × 1, × 2, × 4, or × 8, depending on the level of the signal. Another function of the µC is to control the actuators through its serial peripheral interface, according to the timing diagram establish by the user.

Considering a typical current range from nA to 10 µA and an 18-bit ADC, the resolution of the current measurement circuit is about:

$$\frac{10 \times 10^{-6}\, A}{2^{18}} \cong 40\, pA$$

The voltage measurement circuit depends on the choice of the topology for the measurement of the current because. Thus, when fixing the potential of the WE to mass, the voltage difference between the RE and WE can be measured directly on the RE. To measure the RE voltage, a buffer is used, as is shown in Fig. 6 box (b). The Op OA1 of the voltage measurement circuit must be selected with high input resistance, reduced offset and noise voltage, and the input bias current that must not exceed a few picoamperes. The OA1 output is connected to the inverting input of the CA, and to the PGA. The output PGA is digitally by the 18-bit ADC. It is common to protect the op amp against possible static discharges using a resistance R_p in series to the input of the buffer. Then a capacitor, C_i, is also added in parallel with this resistance to reduce the thermal noise that R_p provides.

The CA is one of the main parts of the amperometric detector that is responsible for maintaining the appropriate constant potential in the cell, V_{CELL}. The CA is aimed at comparing the RE voltage, V_{RE}, with the value of V_{CELL}. Its output is negative feedback through the electrochemical cell and the voltage buffer. Therefore, if both voltages are different, the CA injects a current into the cell to keep V_{RE} constant. The value of V_{CELL} depends on the type of biosensor. It is generated by a 16-bit DAC.

The requirements for the Op are 1) high open-loop gain because this stage is responsible for the main part of the total amplification, 2) high input resistance because we want to use the input as a summing point for both control signals and feedback signals, and 3) high common-mode rejection to prevent noise signals, which are injected simultaneously at both inputs of the operational amplifier.

The scanning rate achieved with this system was evaluated. This parameter, defined as the frequency at which the complete measurement of a sample is carried out, depends on the appropriate operation of the biosensor and the analysis method and settings established from the system configuration. The ethanol concentration is monitored every second in time intervals of 1 h, this being a programmable parameter.

To study the stability of the CA [34], we use the equivalent circuit of the cell modelled before. This makes it possible to check the dynamic response of the regulator to different control requirements. Fig. 7 shows the feedback loop, where $R(s)$ is the function transfer of the regulator circuit, and $H(s)$ is the function transfer of the voltage measurement circuit.

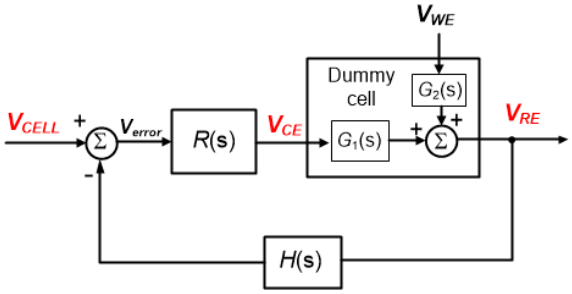

Fig 7. Block diagram of the electrochemical cell control system.

The close loop function transfer is yield by:

$$V_{RE}(s) = V_{CELL}(s)\frac{G_1(s)R(s)}{1 + G_1(s)R(s)H(s)} + V_{WE}(s)\frac{G_2(s)}{1 + G_2(s)R(s)H(s)} \quad (7)$$

The influence of the perturbation V_{WE} can be negligible, therefore:

$$V_{RE}(s) = V_{CELL}(s)\frac{G_1(s)R(s)}{1 + G_1(s)R(s)H(s)} \quad (8)$$

The static and dynamic characteristics of the common analog controllers had been obtained by the means of MATLAB software, and the main conclusions are shown in Table I.

TABLE I
CHARACTERISTICS OF THE CONTROLLERS

Type of controller	$R(s)$	Static Characteristics	Dynamic Characteristics
P	K	Bad	Bad
I	$\frac{1}{sR_cC_1}$	Good	Good
PI	$\frac{1 + sR_1C_1}{sR_cC_1}$	Good	Bad

The best characteristics were obtained by the means of an analog integral controller. Fig. 8 (a) shows its electronic schematic. The dynamic characteristics evaluated were the slew rate and the overshoot. The controller circuit was tested experimentally by feeding a 1 kHz rectangle waveform of a 200-mV amplitude. This is a rather hard test because the control signal in biosensors applications will be a DC signal, generally

one between 0 V and 500 mV. The electrochemical cell was simulated by a dummy cell with different values of capacitors.

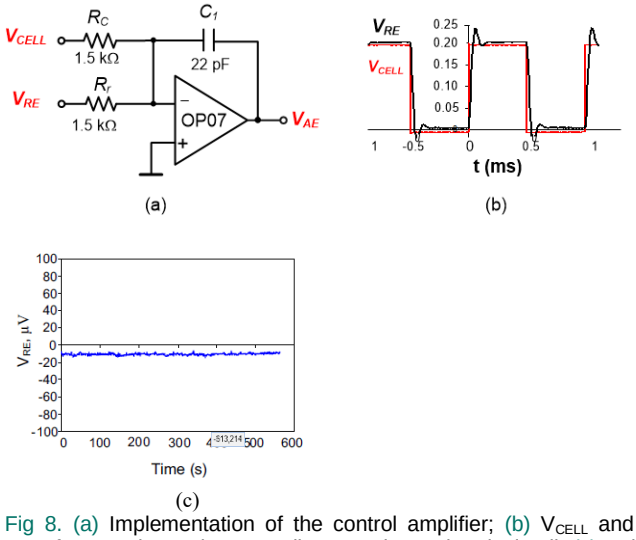

Fig 8. (a) Implementation of the control amplifier; (b) V_{CELL} and V_{RE} waveforms using a dummy cell as an electrochemical cell; (c) Voltage difference between the reference and working electrode. This last electrode is grounded.

The rectangle wave should be transferred to the output with a high slew rate, and oscillations caused by high capacities should be properly damped. These results can be considered as a "good" dynamic characteristic. Fig. 8 (b) shows the waveforms obtained using: $R_1 = 1\ k\Omega$, $R_2 = 10\ k\Omega$, $C_2 = 1\ nF$, $C_1 = 1\ nF$, $R_C = 1.5\ k\Omega$, $R_r = 1.5\ k\Omega$. As can be seen, the slew rate is high, and the oscillations produced by the capacity have a tolerable damping.

The static characteristic evaluated was the accuracy of the control amplifier. The aim was to remain a constant voltage difference between the working and reference electrodes at the selected voltage for each biosensor. In our case, this voltage was 0.00 V. Fig. 8 (c) shows this voltage difference. Its low level is less than 10 µV, does not affect the overall performance of the system, and is below the LSB of the DA converter. This result can be considered as a "good" static characteristic.

2) Drivers of Actuators: The second PCB of the electronics subsystem consists of three blocks: a circuit for extending the microcontroller's number of outputs, an array of Darlington transistors to drive the actuators, and a stage of optocouplers to protect the circuit and avoid noise. These three blocks are shown in Fig. 9.

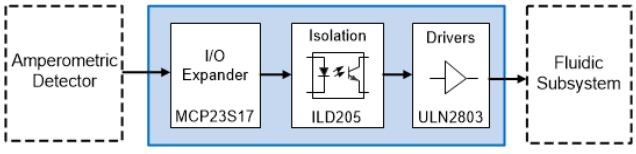

Fig 9. Block diagram of the board to drive the actuators of the fluidic subsystem.

D. Software Application

The software application performs a very important role because all the features of the instrument are controlled by it. The software application enables capturing the data provided by the instrument through a USB port; visualizing the measurements made by the graphical representation of curves; saving, exporting, and importing files; and performing various calculations on the data obtained. One noteworthy aspect is the application's ability to perform calibration on a series of standards and then obtain the measurement of a sample's concentration on the calibration curve.

Fig. 10 shows an example of the user interface main screen. It is divided into several submenus, and some of its options will be disabled while no instrument is connected to the computer. The *Curves* tab shows the curves that are loaded in the software. Selecting each of them will allow actions on the curves. The *Summary* tab shows the concentration and intensity for each standard and sample.

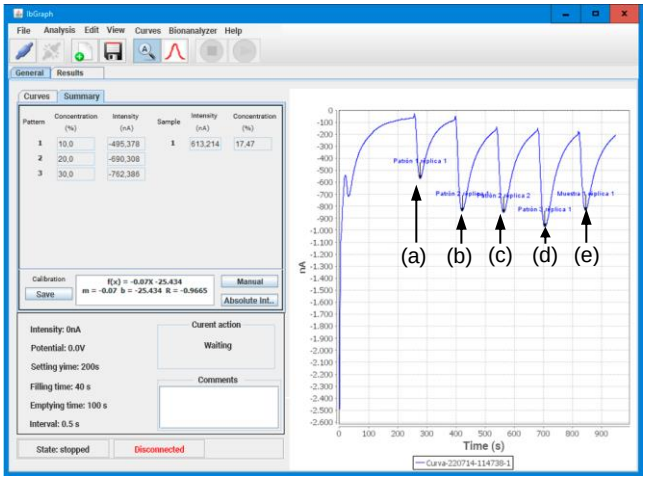

Fig 10. Example of the user interface main screen. (a) Standard 1, replica 1; (b) Standard 2, replica 1; (c) Standard 1, replica 2; (d) Standard 3, replica 1; (e) Sample 1, replica 1.

The *Calibration* window has three buttons: one to save the calculated calibration, one to open the manual mode window, and one to open the absolute intensities window. The manual mode window allows the user to determine the location of each pattern and displays it on the measured curve, rather than the software that determines it automatically. After running the application, it is necessary to physically connect the bioanalyzer to the computer using a USB port. The measurement procedure is as follows:

- Select the option *File*, *New Method* from the menu or press the button on the toolbar. The *Configuration* window shows up, as shown in Fig. 11 (a). In this window, the measurement potential can be selected as well as the amount of time the stabilizing, filling, and emptying phases will last.
- In the *Calibration* tab, Fig. 11 (b), the number of standards to be used in the method, the type of calibration to be used, and the units in which the user prefers the data to be displayed may be selected. For each of the standards, the input of the bioanalyzer may be selected from which the standard, the number of replicates, and the concentration of the standard will be selected.
- In the *Samples* tab, Fig. 11 (c), the number of samples to be analyzed may be selected as well as the input of the bioanalyzer, the number of identical replicas, and the dilution factor of each sample.
- The option *Bioanalyzer*, *Measure*, or the button on the toolbar enable the measurement.

Other features may be accessed via the menu bar, such as

importing and exporting curves to CSV format, editing scales, editing the number of samples to recalibrate, or run cleaning mode. Once the baseline is stabilized, a known amount of standard is added, and the current is expected to restabilize. This last step is repeated three times.

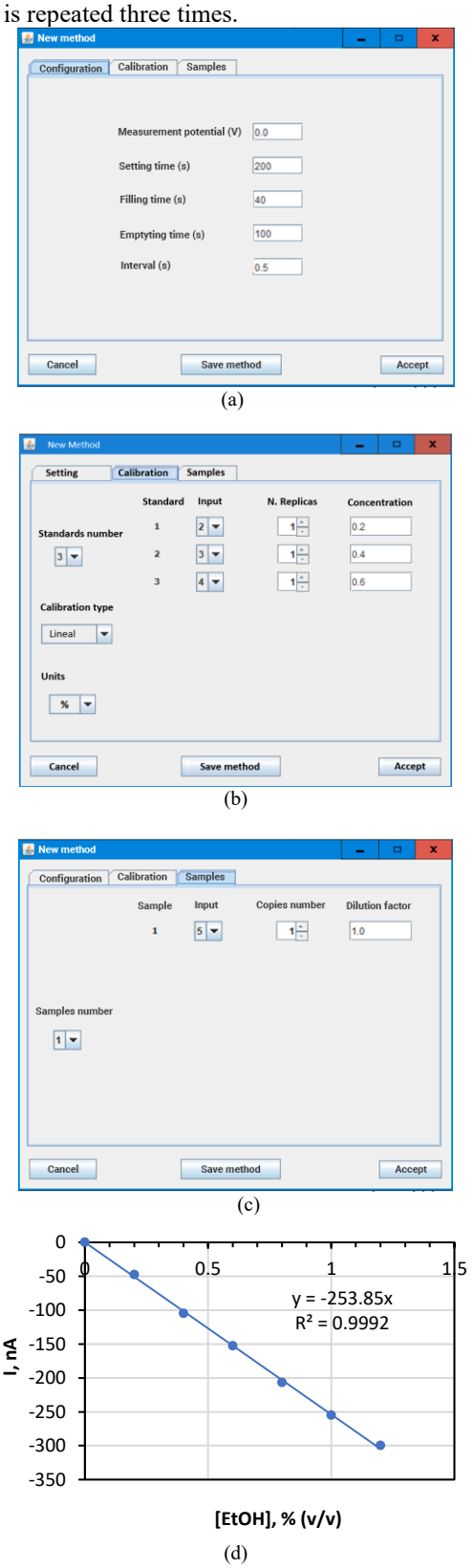

Fig 11. Main screens of the software application: (a) Configuration tab; (b) Calibration tab; (c) Samples tab; (d) Calibration curve.

The magnitude of the current jumps is used for calibration. Fig. 10 (d) shows the calibration curve obtained. It was obtained from data recorder by the software application in CSV format and processed using the Excel program. To obtain the calibration curve, the flow cell is first filled with a carrier solution. After that, a standard of analyte is added, increasing the current. The peak of the current is recorded. After cleaning the cuvette, another standard is added to the flow cell, and the peak current is recorded again. The process is repeated several times. The latest step is to fit the data using the method of least squares. The concentration of analyte in the sample is obtained by interpolating the calibration curve.

III. Results

The developed prototype was tested using an amperometric biosensor [18] for the determination of ethanol in beers with a concentration of <1% (v/v). A stock 20% (v/v) ethanol (Scharlab) solution was prepared in a 0.05 M phosphate buffer of pH 7.4. More diluted standards were prepared by suitable dilution with the same buffer solution, which was also used as a supporting electrolyte. The electrodes were placed in a methacrylate 40 µL cylindrical flow cell. The working conditions were: a) voltage potential applied to the cell 0.0 V, b) flow rate around than 2 ml/min. The software application recorded the current-time curve and the calibration curve, which are shown in Fig. 10 and Fig. 11 (d), respectively. According to the calibration curve, the linear range is between 0.2 and 1.2% (v/v). The limit of detection is 2.3×10^{-2} % (v/v), and quantification is 7.8×10^{-2} % (v/v). These limits were calculated according to $10 \times s_b/m$ criteria, where m is the slope of the calibration graph, and s_b is the standard deviation of the blank current. This was measured each second for 300 seconds before recording the analytical signal (confidence intervals were calculated for $\alpha = 0.05$). The repeatability of the amperometric measurements was evaluated by recording successive measurements of 0.8% (v/v) ethanol standard solutions. The RSD value obtained was 4.5% (n=10). Table II compares the results obtained with those obtained by a reference method using a commercial ethanol amperometric biosensor provided by the company InBea Biosensores S.L.

TABLE II
Evaluation of Ethanol Samples in Beers With Very Low Alcohol Concentrations

Sample	[EtOH], % (v/v), n=3	
	CFA system	Reference Method
1	(0.85 ± 0.02) RSD = 1.9%	(0.82 ± 0.07) RSD = 3.7%
2	(0.94 ± 0.02) RSD = 2.9%	(0.90 ± 0.08) RSD = 3.3%
3	(0.89 ± 0.02) RSD = 1.7%	(0.87 ± 0.05) RSD = 2.2%
4	(0.85 ± 0.05) RSD = 4.9%	(0.90 ± 0.03) RSD = 2.7%
5	(0.92 ± 0.03) RSD = 2.8%	(0.91 ± 0.04) RSD = 3.9%

Fig. 12 shows the placement of the components inside the instrument. To obtain good results the following issues should be considered:

1) The flow cell was placed outside of the enclosure over a metallic arm. The aim is to avoid stray fields from the

actuators. Longer cables affect the dynamic response of the system.

2) To fix the pumps and valves in the enclosure, an E-shaped block was designed and built using high-density black PVC, as can be seen in the center of Fig. 11. The solenoid valves were connected using a silicone tube with a 5 mm diameter. For the external connections and the passage of valves to pumps, a Teflon (PTFE) pipe with a diameter of 2 mm was used. The coupling between tubes was made from metal flanges. This configuration prevents the loss of pressure and the entry of air into the circuit.
3) Avoiding noise and interference is critical in the design of an electrochemical cell. The CE is the least critical, so there is no need to shield it. Shielding may increase the parasitic capacitance affecting the dynamic response of the system. The WE is virtually connected to a constant potential that is prone to picking up noise, so it should be shielded. The RE input of the amperometric detector has a high input resistance. The current never exceeds a few picoamperes, so it can pick up noise from the AC line or RF frequencies. To avoid capacitive loads between the RE cable and its shield, never connect this shield to the ground.
4) Considering the operational characteristics of the prototype, the high working flow rate provided by the peristaltic pumps (2.0 ml/min) implied the consumption of a large volume of carrier solution. Therefore, the recirculation of the outlet from the flow cell into the carrier solution should be implemented, significantly decreasing the waste of the carrier solution.
5) The high content of dissolved gas in beer may cause irreproducibility in the ethanol diffusion process through the membrane, generating considerable variations of the analytical response. To overcome this limitation, a de-bubbler unit should be incorporated between the sampling and the inlet to the continuous flow system.

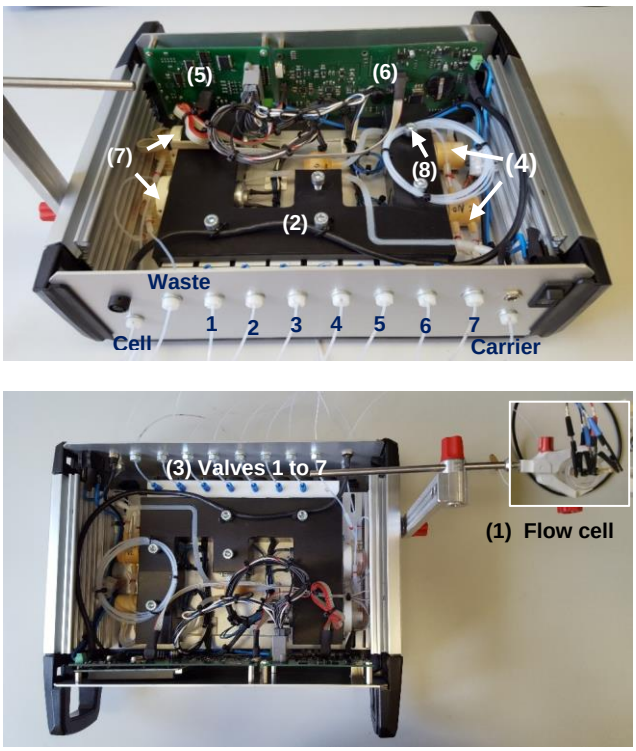

Fig 12. CFA system prototype: (1) the electrochemical flow cell; (2) the PVC module to fix the valves and pumps: (3) Valves 1 to 7; (4) Valves 8, 9, and 10; (5) Electronic board to activate the valves and pumps; (6) Electronic board of the amperometric detector; (7) Pumps 1 and 2; (8) Loop.

IV. Conclusion

This work reports the development of an automated continuous flow system based on amperometric biosensors that can be used as a bioanalyzer. All features of the instrument were controlled by the software application. The tests were made using an ethanol amperometric biosensor to obtain the calibration curves for alcohol concentrations below 1.0% (v/v). The relative standard deviation value obtained was 4.5% (n=10), and the limit of detection was 2.3×10^{-2} % (v/v). By changing the configuration of the parameters of the application and the type of biosensor to one that is specific to the target analyte, this system can be applied to other analytes of interest. The test proved to be an excellent basis for online analysis and could be part of an integrated control system. The average response time of the system was 3 minutes, which allowed us to measure 20 samples per hour.

References

[1] K. Cammann, "Biosensors based on ion-selective electrodes," *Fresen Z Anal Chem*., no. 287, pp. 1–9, Jan.1977.
[2] D.R.Thevenot, K. Toth, R.A. Durst, G.S. Wilson. "Electrochemical biosensors: recommended definitions and classification," *Biosens Bioelectron*. no.16, pp. 121–131. 2001.
[3] S. Borgmann, A. Schulte, S. Neugebauer, W. Schuhmann, Advances in Electrochemical Science and Engineering. vol. 13, chapter 1, Wiley-VCH Verlag GmbH & Co. KGaA, Weinheim. 2012, pp. 1–38.
[4] M. Trojanowicz, "Flow Injection Analysis: Instrumentation and Applications," World Scientific Publishing Co. Singapore. 2000.
[5] L. Moreno, A. Baldi, A. Merlos, N. Abramova, A. Ipatov, C. Jiménez, A. Bratov, "Integrated Multisensor for FIA-Based Electronic Tongue Applications," IEEE Sensors Journal, vol. 8, no. 5, pp. 608 – 615, May 2008.
[6] L. Celio, M. Ottaviani, R. Cancelliere, A. D. Tinno, P. Panjan, A.M. Sesay, L. Micheli, "Microfluidic Flow Injection Immunoassay System for Algal Toxins Determination: A Case of Study," *Front. Chem.*: 626630. pp. 1–12, March 2021.
[7] F.R.P. Rocha, E.A.G. Zagatto, "Flow analysis during the 60 years of Talanta," *Talanta*, vol. 206, no. 120185, pp. 1–7, Jan. 2020.
[8] R. Ishimatsu, S. Shimizu, S. Hongsibsong, K. Nakano, C. Malasuk, Y. Oki, K. Morita, "Enzyme-linked immunosorbent assay based on light absorption of enzymatically generated aniline oligomer: flow injection analysis for 3-phenoxybenzoic acid with anti-3-phenoxybenzoic acid monoclonal antibody," *Talanta*, vol. 218, 121102. pp. 1–9, Oct. 2020.
[9] M.A. Kumar, M.A. Mazlomi, M. Hedström, B. Mattiasson, "Versatile automated continuous flow system (VersAFlo) for bioanalysis and bioprocess control," *Sens. and Acts. B*, no. 161, pp. 855–861, 2012.
[10] E. Vargas, M.A. Ruiz, F.J. Ferrero, S. Campuzano, V. Ruiz-Valdepeñas, A.J. Reviejo, J.M. Pingarrón, "Automatic bionalyzer using an integrated amperometric biosensor for the determination of L-malic acid in wines," *Talanta*, no. 158, pp. 6–13, 2016.
[11] R.A.S. Lapa, J.L.F.C. Lima, I.V.O.S Pinto, "Development of a sequential injection analysis system for the simultaneous biosensing of glucose and ethanol in bioreactor fermentation," *Food Chemistry*, vol. 81, no. 1, pp. 141–146, 2003.
[12] B. Wibowotomo, J.-B Eun, J. Rhee, "Development of a Sequential Injection Analysis System for the Determination of Saccharin," *Sensors*, vol. 17, no. 2891. pp. 1–10, 2017.
[13] F.R.P. Rocha, P.B. Martelli, B.F. Reis, "A multicommutation-based flow system for multi-element analysis in pharmaceutical preparations," *Talanta*, vol. 55, no. 4, pp. 861–869. Dec. 2001.
[14] E.J. Llorent-Martínez, P.O. Barrales, M.L. Fernández-de Córdova, A. Ruiz-Medina, "Multicommutation in Flow Systems: A Useful Tool for

Pharmaceutical and Clinical Analysis," *Current Pharm. Anal*. 6, pp. 53–65, 2010.

[15] A.R. Molina, E.V. Alonso, M.T. Siles, A.G. Torres, J.M. Cano, "Spectrophotometric Flow Injection Method for Determination of Sorbic Acid in Wines," John Wiley & Sons, Inc. LRA, 11, pp. 299–303. 1999.

[16] H. Saito, T. Nakazato, N. Ishi, H. Kudo, K. Otsuka, H. Endo, K. Mitsubayashi, "An optical flow injection analysis system for measurement of glucose in tomato," *Eur Food Res Technol*, no. 227, pp. 473–478. 2008.

[17] A.M. Titoiu, G. Necula-Petrareanu, D. Visinescu, V. Dinca, A. Bonciu, C.N. Mihailescu, C. Purcarea, R. Boukherroub, S. Szunerits, A. Vasilescu "Flow injection enzymatic biosensor for aldehydes based on a Meldola Blue-Ni complex electrochemical mediator," *Microchim Acta*, vol. 187, no. 550, Sep. 2020.

[18] E.H. Hansen, M. Miró, "Flow Injection Analysis in Industrial Biotechnology," in *Encyclopedia of Industrial Biotechnology*; John Wiley & Sons: Hoboken, NJ, USA, 2009.

[19] A. Guzmán-Vázquez de Prada, N. Peña, M.L. Mena, A.J. Reviejo, J.M. Pingarrón, "Graphite–Teflon composite bienzyme amperometric biosensors for monitoring of alcohols," *Biosens and Bioelects*., vol. 18, no. 10, pp. 1279–1288. Sep. 2003.

[20] N. Peña, G. Ruiz, A.J. Reviejo, J.M. Pingarrón, "Graphite−Teflon Composite Bienzyme Electrodes for the Determination of Cholesterol in Reversed Micelles," Application to Food Samples. *Anal. Chem*., vol. 73, no. 6, pp. 1190–1195. Feb. 2001.

[21] B. Serra, A.J. Reviejo, C. Parrado, J.M. Pingarrón, "Graphite-Teflon composite bienzyme electrodes for the determination of L-lactate: application to food samples," Biosens & Bioelectronics, vol. 14, no. 5, 505–513. Sep. 1999.

[22] Disposable amperometric biosensor, production method thereof and method for determining the presence of analytes in foods, by A.J. Reviejo, J.M. Pingarrón, S. Campuzano, M. Gamella, V. Vicente, Manso, F.J. Ferrero, J.C. Campo, M. Valledor (2010, January 28). Patent PCT/ES2009/000381. [Online]. Available: Google Patents.

[23] Basics of Electrochemical Impedance Spectroscopy, [Online]. Available: http://www.gamry.com.

[24] Gamry Instruments Inc., Potentiostat Primer. [Online]. Available: http://www.gamry.com/.

[25] Bank Elektronik, Introduction to Potentiostats. [Online]. Available: http://www.bank-ic.de/.

[26] J.P. Villagrasa, J. Colomer-Farrarons, P.L. Miribel, "Bioelectronics for Amperometric Biosensors". Chapter 2013. [Online:]. Available: https://www.intechopen.com/chapters/43463.

[27] J.R. Blanco, F.J. Ferrero, J.C. Campo, J.C. Antón, J.M. Pingarrón, A.J. Reviejo, J. Manso, "Design of a Low-Cost Portable Potentiostat for Amperometric Biosensors," in Proc. *IEEE Instrumentation and Measurement Technology Conference (I2MTC)*, Sorrento, Italy, 2006, pp. 24–27.

[28] S. Kwakye, A. Baeumner, "An embedded system for portable electrochemical detection," *Sens. and Acts. B*, no. 123, pp. 336–343, 2007.

[29] G. Rocchitta, R. Migheli, S. Dedola, G. Calia, M.S. Desole, E. Miele, J.P. Lowry, R.D. O'Neill, P.A. Serra, "Development of a distributed, fully automated, bidirectional telemetry system for amperometric microsensor and biosensor applications," *Sens. and Acts. B*, vol. 126, pp. 700–709. 2007.

[30] W-S Wang, W-T Kuo, H-Y Huang, C-H Luo, "Wide Dynamic Range CMOS Potentiostat for Amperometric Chemical Sensor," *Sensors*, vol. 10, pp. 1782–1797, March 2010.

[31] S.M. Martin, F.H. Gebara, T.D. Strong, R. B. Brown, "A Fully Differential Potentiostat," *IEEE Sensors Journal*, vol. 9, no. 2, pp. 135–142, Feb. 2009.

[32] P. Lopin, K.V. Lopin, "PSoC-Stat: A single chip open source potentiostat based on a Programmable System on a Chip," *PLoS ONE*, vol. 13, no. 7. pp. 1–21, July 2018.

[33] V. Bianchi 1, A. Boni, M. Bassoli, M. Giannetto, S. Fortunati, M. Careri, I. de Munari, "IoT and Biosensors: A Smart Portable Potentiostat with Advanced Cloud-Enabled Features," *IEEE Access*, vol. 9, pp. 141544–141554, Oct. 2021.

[34] S.M. Rezaul, "Stability Analysis and Novel Compensation of a CMOS Current-Feedback Potentiostat Circuit for Electrochemical Sensors," *IEEE Sensors Journal*, vol. 7, no. 5, 814–824, May 2007.